the plant journal

SEB Society for Experimental Biology

*The Plant Journal* (2015) **83,** 783–793 doi: 10.1111/tpj.12925

# Exploring diterpene metabolism in non-model species: transcriptome-enabled discovery and functional characterization of labda-7,13*E*-dienyl diphosphate synthase from *Grindelia robusta*

**Philipp Zerbe[1,2,*], Selina M. Rodriguez[1], Sibongile Mafu[1], Angela Chiang[2], Harpreet K. Sandhu[2], Mark O'Neil-Johnson[3], Courtney M. Starks[3] and Jörg Bohlmann[2]**

[1]*Department of Plant Biology, University of California-Davis, 1 Shields Avenue, Davis, CA 95616, USA,*
[2]*Michael Smith Laboratories, University of British Columbia, 2185 East Mall, Vancouver, BC V6T 1Z4, Canada, and*
[3]*Sequoia Sciences, 1912 Innerbelt Business Center Drive, Saint Louis, MO 63114, USA*

Received 5 May 2015; revised 16 June 2015; accepted 19 June 2015; published online 28 June 2015.
*For correspondence (e-mail pzerbe@usdavis.edu).

## SUMMARY

***Grindelia robusta*** **or gumweed, is a medicinal herb of the sunflower family that forms a diverse suite of diterpenoid natural products. Its major constituents, grindelic acid and related grindelane diterpenoids accumulate in a resinous exudate covering the plants' surfaces, most prominently the unopened composite flower. Recent studies demonstrated potential pharmaceutical applications for grindelic acid and its synthetic derivatives. Mining of the previously published transcriptome of *G. robusta* flower tissue identified two additional diterpene synthases (diTPSs). We report the *in vitro* and *in vivo* functional characterization of an *ent*-kaurene synthase of general metabolism (GrTPS4) and a class II diTPS (GrTPS2) of specialized metabolism that converts geranylgeranyl diphosphate (GGPP) into labda-7,13*E*-dienyl diphosphate as verified by nuclear magnetic resonance (NMR) analysis. Tissue-specific transcript abundance of *GrTPS2* in leaves and flowers accompanied by the presence of an endocyclic 7,13 double bond in labda-7,13*E*-dienyl diphosphate suggest that GrTPS2 catalyzes the first committed reaction in the biosynthesis of grindelic acid and related grindelane metabolites. With the formation of labda-7,13*E*-dienyl diphosphate, GrTPS2 adds an additional function to the portfolio of monofunctional class II diTPSs, which catalytically most closely resembles the bifunctional labda-7,13*E*-dien-15-ol synthase of the lycopod *Selaginella moellendorffii.* Together with a recently identified functional diTPS pair of *G. robusta* producing manoyl oxide, GrTPS2 lays the biosynthetic foundation of the diverse array of labdane-related diterpenoids in the genus *Grindelia.* Knowledge of these natural diterpenoid metabolic pathways paves the way for developing biotechnology approaches toward producing grindelic acid and related bioproducts.**

**Keywords: diterpenoid biosynthesis, diterpene synthase, *Grindelia robusta*, medicinal plants, plant-specialized metabolism, grindelic acid, plant natural products.**

## INTRODUCTION

Mankind has utilized the metabolic diversity of medicinal plants for millennia. Today, plant natural products are of increasing importance as a resource for traditional pharmacopeias and the production of advanced plant-based or semi-synthetic drugs (Harvey *et al.*, 2015). Advanced genomics and metabolomics approaches enable identification of the biosynthetic genes, enzymes and pathways across the biodiversity of non-model plant species with medicinal or other industrial relevance (Facchini *et al.*, 2012; Higashi and Saito, 2013; Zerbe *et al.*, 2013). Combined with progress in the field of metabolic engineering this knowledge can be translated into developing biomanufacturing platforms for production and commercialization of plant-derived bioactive metabolites. Labdane-related diterpenoids form a large group of more than 10 000 different compounds (Peters, 2010), many of which are of ecological and industrial impor-

tance. While a few labdane diterpenoids, such as gibberellin phytohormones, function in general (i.e. primary) metabolism, most diterpenoids represent specialized (i.e. secondary) metabolites that are often species-specific and play critical roles in the ecological interaction of plants with their environment (Keeling and Bohlmann, 2006a; Gershenzon and Dudareva, 2007; Hanson, 2011). Many of these specialized diterpenoids also serve as important pharmaceuticals, food additives, fragrance components and other commercial bioproducts (Bohlmann and Keeling, 2008; Hanson, 2011; Zerbe and Bohlmann, 2015a).

Species of the genus *Grindelia* (Asteraceae) produce copious amounts of a resinous exudate that is secreted through specialized ducts and glandular trichomes and accumulates on the surface of leaves, stems and involucres of flowers (Ahmed *et al.*, 2001; Ybarra *et al.*, 2005), lending the genus its common name gumweed (Figure 1). This resin contains a suite of labdane diterpenoids, comprising manoyl oxide-derived metabolites (Bohlmann *et al.*, 1982; Bartoli *et al.*, 2011), and an array of grindelane-type diterpenoids with grindelic acid as signature metabolite of the genus (Ahmed *et al.*, 2001).

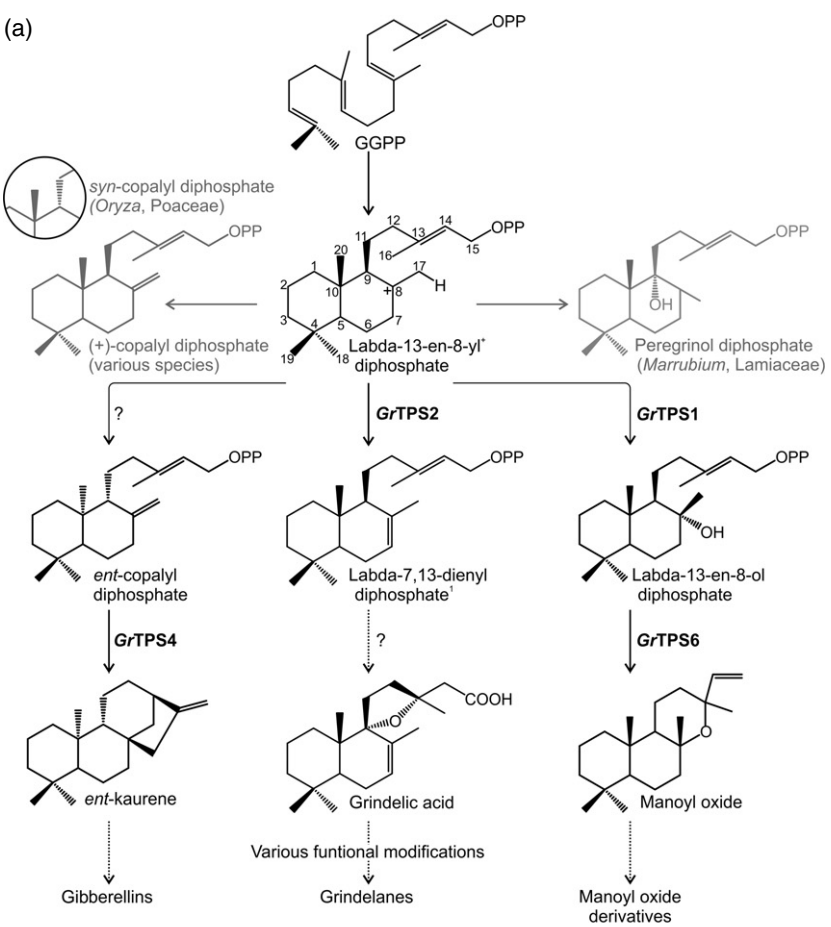


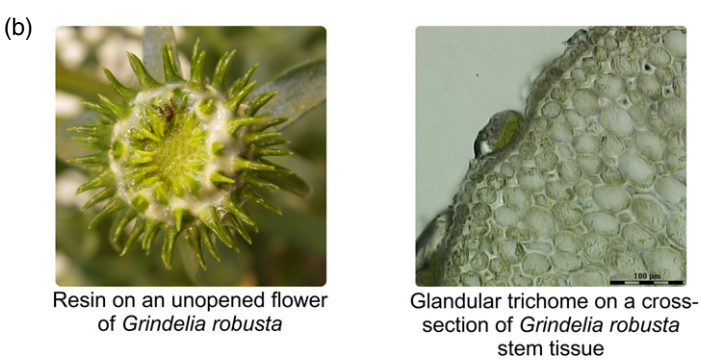


**Figure 1.** Diterpenoid biosynthesis in *Grindelia robusta.*
(a) Biosynthesis of labdane-related diterpenoids in angiosperms requires the sequential activity of monofunctional class II and class I diterpene synthases (diTPSs). Class II diTPSs convert the precursor geranylgeranyl diphosphate (GGPP) in to a variety of bicyclic prenyl diphosphate intermediates via a common labda-13-en-8-yl$^{+}$ diphosphate intermediate. Class I diTPSs transform these bicyclic intermediates into an array of distinct diterpene scaffolds. In *Grindelia robusta* (Asteraceae), GrTPS1, GrTPS6 and GrTPS2 form the gateway to the biosynthesis of specialized diterpenoids, including *ent*-kaurene en route to gibberellin phytohormones, manoyl oxide derived metabolites and the family of grindelane diterpenoids with grindelic acid as major constituent. On account of its structural similarity to grindelic acid, labda-7,13*E*-dienyl diphosphate represents a key intermediate in the formation of grindelanes with GrTPS2 catalyzing the committed reaction step.
(b) *G. robusta* produces large quantities of these diterpenoids that are secreted through specialized ducts and glandular trichomes as a resinous exudate that covers the surface of the aerial parts of the plant.

Members of the genus are native to the Americas and have been used as herbal remedies for their sedative and anti-inflammatory properties, and the treatment of asthmatic ailments and poison ivy dermatitis. Potential applications in cancer therapy and the treatment of Alzheimer's disease have recently been demonstrated for natural grindelane compounds and synthetic derivatives thereof (Reta *et al.*, 2013; Alza *et al.*, 2014). Knowledge of the genes and enzymes for grindelic acid biosynthesis would extend our understanding of diterpenoid metabolic diversity and can provide the means for bioengineering of grindelane-type molecules.

Plant diterpenoids predominantly originate from the 2-*C*-methyl-erythritol-4-phosphate (MEP) pathway with geranylgeranyl diphosphate (GGPP) as general precursor (Peters, 2010). Downstream of GGPP, diterpenoid biosynthesis follows a modular pattern involving the activity of different combinations of diterpene synthases (diTPSs), cytochrome P450 dependent monooxygenases (P450s), and a few other enzyme classes to generate the diversity of natural diterpenoids (Peters, 2010; Chen *et al.*, 2011; Nelson and Werck-Reichhart, 2011; Zerbe *et al.*, 2013; Zerbe and Bohlmann, 2015b). DiTPSs catalyze the initial conversion of GGPP via carbocation-driven multistep cyclization and rearrangement reactions to form a large array of acyclic or cyclic diterpene scaffolds (Davis and Croteau, 2000; Peters, 2010; Chen *et al.*, 2011; Zerbe *et al.*, 2013). In angiosperms, labdane-related diterpenoids are formed by the consecutive activity of two monofunctional diTPSs, which act as pairs of class I and class II enzymes. Class II and class I diTPSs belong to the TPS-c and TPS-e/f clades of the large TPS superfamily, respectively (Peters, 2010; Chen *et al.*, 2011). Class II diTPSs catalyze the initial protonation-dependent cyclization of GGPP into bicyclic prenyl diphosphates, which are then converted by class I diTPSs through ionization of the diphosphate moiety and various possible rearrangements to afford diterpene scaffolds of distinct stereochemistry and in select cases position-specific oxygenation.

The class II reaction proceeds via a common labda-15-en-8-yl$^{+}$ diphosphate intermediate that may undergo a variety of reactions to form different prenyl diphosphates (Figure 1). Deprotonation of the carbocation at carbon C-8 affords *ent*(9*R*,10*R*)-copalyl diphosphate (*ent*-CPP) as an essential intermediate in gibberellin biosynthesis of all vascular plants (Keeling *et al.*, 2010; Peters, 2010). Distinct conformation of the GGPP substrate prior to deprotonation leads to the formation of CPP isomers with normal (9*S*,10*S*) or *syn* (9*S*,10*R*) stereochemistry involved in the biosynthesis of various specialized diterpenoids in both, angiosperms and gymnosperms (Keeling and Bohlmann, 2006b; Xu *et al.*, 2007; Zerbe *et al.*, 2013; Brückner *et al.*, 2014; Pateraki *et al.*, 2014). Furthermore, hydride or methyl migrations may occur to afford double bond isomers of CPP, such as labda-7,13-dienyl diphosphate (Mafu *et al.*, 2011). In addition, water capture of the carbocation at C-8 or C-9 can occur prior to deprotonation, leading to oxygenated CPP variants found in numerous taxa (Falara *et al.*, 2010; Sallaud *et al.*, 2012; Zerbe *et al.*, 2012, 2014; Pateraki *et al.*, 2014). Formation of labda-7,13*E*-dienyl diphosphate is thus far only known from the lycophyte *Selaginella moellendorffii* as an intermediate of the bifunctional class I/II diTPS SmCPSKSL1 which converts the prenyl diphosphate intermediate into labda-7,13*E*-dien-15-ol (Mafu *et al.*, 2011). Such bifunctional class I/II diTPSs to current knowledge only exist in lower plants and conifers, but are not known in angiosperms (Zerbe and Bohlmann, 2015b).

Based on the structural similarity of labda-7,13*E*-dien-15-ol and grindelic acid containing a characteristic 7,8 double bond, it can be proposed that a class II diTPS forming labda-7,13*E*-dienyl diphosphate would be a key enzyme in the biosynthesis of grindelane diterpenoids. We tested this hypothesis and report here the functional characterization of two diTPSs from *G. robusta*, an *ent*-kaurene synthase (GrTPS4) and a labda-7,13*E*-dienyl diphosphate synthase (GrTPS2).

## RESULTS

### Tissue-specific terpenoid profiles of *Grindelia robusta*

To investigate the spatial distribution of terpenoids in *G. robusta*, we analyzed the mono- sesquiterpenoid and diterpenoid content and composition of extracts of roots, stems, leaves, flowers and resin from flower involucres via gas chromatography/mass spectrometry (GC/MS) analysis. Consistent with previous phytochemical studies on species of *Grindelia* (Bohlmann *et al.*, 1982; Fraternale *et al.*, 2007; Veres *et al.*, 2014), terpenoids were almost exclusively present in the aerial parts of the plant (Figure 2 and Table S1). Among the diterpenoids, grindelic acid was the predominant metabolite and most abundant in resin with 9-, 37-, and 81-fold higher levels as compared with flowers, leaves and stems, respectively. In addition, manoyl oxide (most abundant in flowers and resin), two grindelane-type diterpenoids that could not be unambiguously identified, and several monoterpenoid and sesquiterpenoids were detected. Notably, manoyl oxide and grindelic acid, albeit in trace amounts, were also observed in root tissue. Head space GC/MS analysis of terpenoids emitted from intact flowers and leaves identified α- and β–pinene, myrcene, limonene, borneol and germacrene D as major volatile constituents of *G. robusta*, the latter also abundant in tissue extracts.

### Identification of diterpene synthases in *Grindelia robusta*

In an earlier study we reported the discovery of six diTPS candidates (TPS1–6) from *G. robusta* using a combination

 

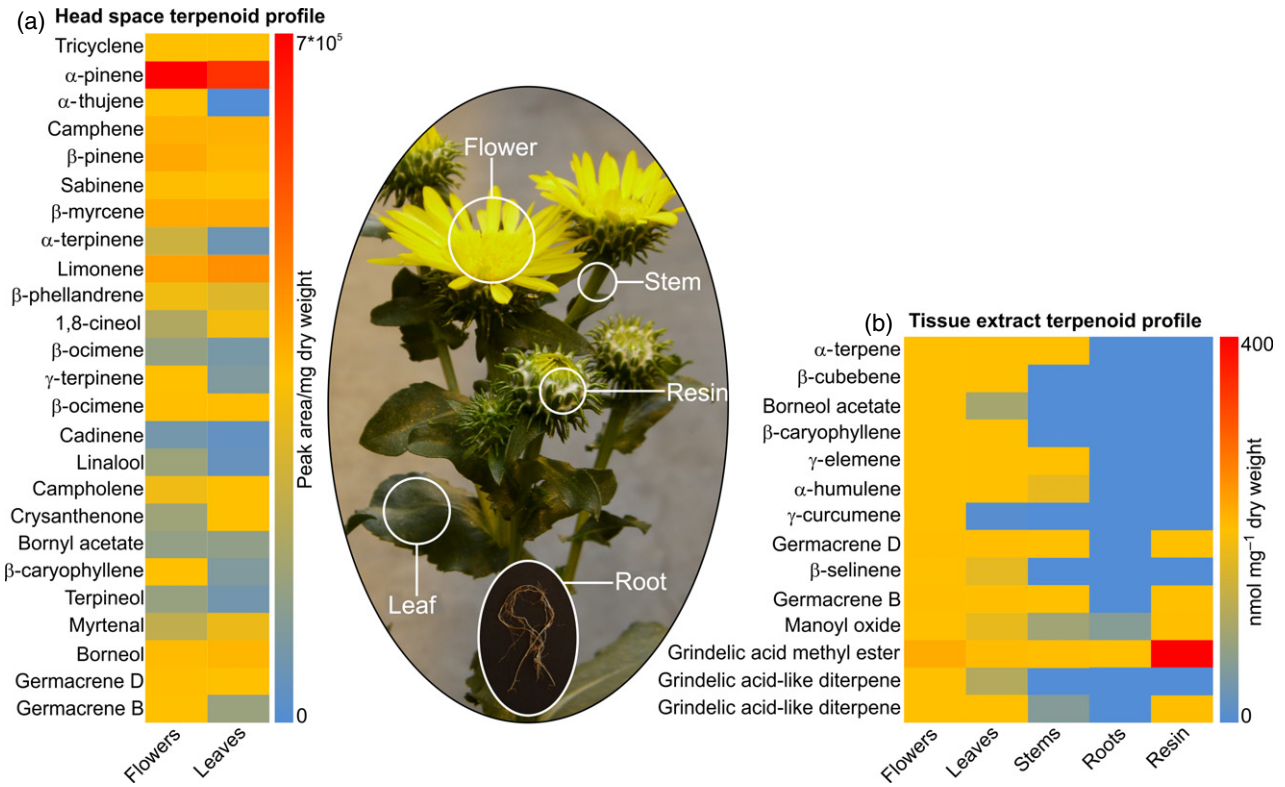


**Figure 2.** Organ-specific terpenoid profile of *Grindelia robusta*.
(a) Heatmap showing abundance of terpenoids detected in leaves, stems, flowers, roots and resin of *G. robusta*. Metabolites were isolated by head space analysis and organic solvent extraction of ground tissues, and subsequent GC/MS analysis. Compound identification is based on significant matches to reference mass spectra databases of the National Institute of Standards and Technology (NIST) MS library searches (Wiley W9N08L).
(b) Terpenoids isolated by liquid extraction were quantified based on 1-eicosene as internal standard ($n = 3$). Detailed results of the quantitative analysis are given in Table S1.

of *de novo* transcriptome sequencing of flower tissue, and computational and biochemical functional gene discovery approaches (Zerbe *et al.*, 2013). Three diTPSs were biochemically characterized, including a class II diTPS (GrTPS1) converting GGPP into labda-13-en-8-ol diphosphate (LPP), and two class I diTPSs which form manoyl oxide from LPP (GrTPS6), and geranyllinalool from GGPP (GrTPS5). However, these functions did not account for an enzyme of grindelic acid biosynthesis as the major metabolite in *G. robusta*, leading us to an in-depth investigation of the three additional diTPS candidates GrTPS2, GrTPS3 and GrTPS4. The sequence of GrTPS2 resembles a class II diTPS with the characteristic DxDD catalytic motif, and GrTPS4 represents a γβα-domain class I diTPS harboring the C-terminal DDxxD and NSE/DTE signature motifs. GrTPS3 was identified as a short transcript fragment with similarity to a class II diTPS, but despite extensive RACE-PCR experiments the full-length sequence could not be obtained (Figure S1), and was hence excluded from further functional analysis. Phylogenetic analysis placed GrTPS4 into the TPS-e/f clade of the TPS family (Figure 3). Among the known Asteraceae diTPSs, GrTPS4 groups together with *ent*–kaurene synthases from *Lactuca sativa*, *Helianthus annuus* and *Stevia rebaudiana* (Richman *et al.*, 1999; Sawada *et al.*, 2008; Pugliesi *et al.*, 2011), suggesting a similar or identical catalytic function. In contrast, GrTPS2 belongs to the TPS-c family of class II diTPSs and is phylogenetically distant from known Asteraceae *ent*–CPP synthases, forming a subgroup with an uncharacterized class II diTPS from *Stevia ovata* and the LPP synthase GrTPS1, supporting a role in specialized metabolism. However, with a protein sequence identity of only 55% GrTPS1 and GrTPS2 are likely to catalyze different diTPS reactions.

### Functional characterization of GrTPS2 and GrTPS4

To functionally characterize GrTPS2 and GrTPS4, the FL sequence of GrTPS4 and a truncated sequence of GrTPS2 (lacking the first 47 N-terminal amino acids representing the plastidial transit peptide) were cloned into the plasmid pET28b(+) and expressed in *Escherichia coli* BL21DE-C41 cells, followed by $Ni^{2+}$NTA-affinity purification of the recombinant proteins. Based on its sequence annotation as a class II diTPS, GrTPS2 was assayed with GGPP as a substrate and subsequent analysis of the reaction products by liquid chromatography-mass spectrometry with electrospray ionization (LC-ESI-MS) in negative mode. The

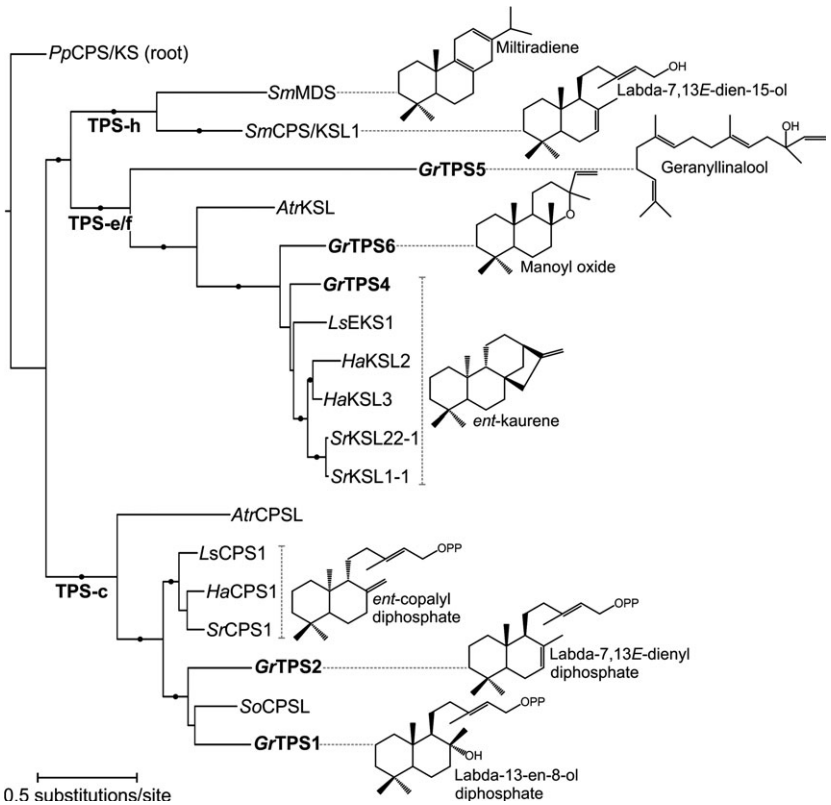


**Figure 3.** Phylogeny of Asteraceae diterpene synthases.
Maximum-likelihood tree illustrating the phylogeny of known Asteraceae diterpene synthases of the TPS-c and TPS-e/f clades in relation to ancestral enzymes from *Amborella trichopoda* and *Physcomitrella patens ent*-kaurene/kaurenol synthase, the latter used to root the tree. Branches with bootstrap support of >75% (1000 repetitions) are highlighted. Abbreviations and accession numbers: AtrCPSL, *Amborella trichopoda* putative *ent*-copalyl diphosphate (CPP) synthase (XP_006838249); AtrKSL, *A. trichopoda* putative *ent*-kaurene synthase (XM_006853432); GrTPS1, *Grindelia robusta* labda-13-en-8-ol diphosphate (LPP) synthase (KC7022400); GrTPS2, *G. robusta* labda-7,13*E*-dienyl diphosphate synthase (KR089902); GrTPS4, *G. robusta ent*-kaurene synthase (KR089903); GrTPS5, *G. robusta* geranyllinalool synthase (KC7022401); GrTPS6, *G. robusta* manoyl oxide synthase (KC7022399); HaCPS1, *Helianthus annuus ent*-CPP synthase (FN689857); HaKSL2, *H. annuus ent*-kaurene synthase 2 (FN689858); HaKSL3, *H. annuus ent*-kaurene synthase 3 (FN689859); LsCPS1, *Lactuca sativa ent*-CPP synthase 1 (BAB12440); LsEKS1, *Lactuca sativa ent*-kaurene synthase 1 (BAB12441); PpCPS/KS, *Physcomitrella patens ent*-(hydroxy)-kaurene synthase (BAF61135); SmMDS, *Selaginella moellendorffii* miltiradiene synthase (BAL41682); SmCPSKSL1, *S. moellendorffii* labda-7,13*E*-dien-15-ol synthase (AEK75338); SoCPSL, *Stevia ovate* putative *ent*-CPP synthase (AER58181); SrCPS1, *Stevia rebaudiana ent*-CPP synthase (AF034545); SrKSL1-1, *S. rebaudiana ent*-kaurene synthase 1 (AF097310); SrKSL22-1, *S. rebaudiana ent*–kaurene synthase 2 (AF097311).

*Gr*TPS2 product showed an identical retention time (7.6 min) and parent mass of *m*/*z* 449 as compared with *ent*-CPP formed by the *Zea mays ent*-CPP synthase (Harris *et al.*, 2005), indicating that GrTPS2 produces a CPP-type prenyl diphosphate (Figure 4). However, a detailed comparison of the obtained mass spectra revealed minor differences in the fragmentation patterns of the *Gr*TPS2 product and *ent*-CPP, suggesting that GrTPS2 forms a distinct product. GC/MS analysis of the dephosphorylated product showed that the GrTPS2 product has a retention time that is different from *ent*-CPP (12.7 min and 11.7 min, respectively; Figure 5). With mass ions of *m*/*z* 204(100), 189(20), 161(29), 135(25), 109(48) and 81(40) the fragmentation pattern of the dephosphorylated GrTPS2 product showed high similarity to labda-7,13*E*-dien-15-ol formed by the bifunctional class I/II diTPS SmCPSKSL1 isolated from *S. moellendorffii* (Mafu *et al.*, 2011). A second minor compound detected in the product profile of GrTPS2 (Figure 5a, peak 2) also showed highly similar mass spectral characteristics as labda-7,13*E*-dien-15-ol and may represent a degradation product resulting from the heated GC conditions as described for other class II diTPSs (Zerbe *et al.*, 2012, 2014). To verify the identity of the GrTPS2 product, larger-scale assays were performed to afford product amounts suitable for nuclear magnetic resonance (NMR) analysis. Following product purification by chromatography on a silica matrix, 1D and 2D NMR spectra were acquired, which identified the dephosphorylated GrTPS2 product as labda-7,13*E*-dien-15-ol (Figure 5b). Together, these results confirmed GrTPS2 as a monofunctional labda-7,13*E*-dienyl diphosphate synthase, which adds an additional function to the known plant class II diTPSs. Previously characterized plant class II diTPSs include enzymes for the formation of *ent*-CPP, *syn*-CPP, normal CPP [i.e. (+)-CPP], LPP and peregrinol diphosphate (for review see Zerbe and Bohlmann, 2015b).

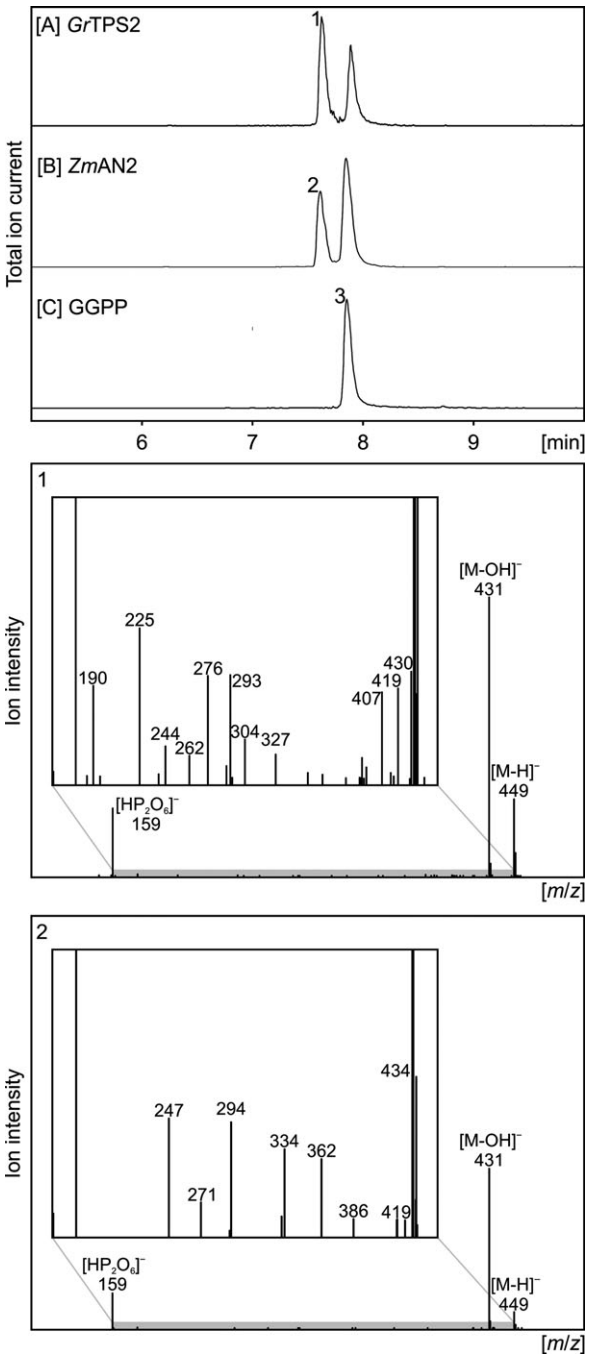


**Figure 4.** LC/MS analysis of the GrTPS2 reaction product.
Normal phase LC/MS analysis with electrospray ionization (ESI) in negative mode was used to detect class II diTPS reaction products from GGPP as substrate without dephosphorylation. Results are depicted as extracted ion chromatograms (EIC) of the parent mass *m/z* 449 corresponding to a non-oxygenated bicyclic prenyl diphosphate product. The GrTPS2 product (a) is shown in comparison with *ent*-CPP produced by the *Zea mays ent*-CPP synthase (ZmAN2, (Harris *et al.*, 2005) (b) and GGPP alone (c). Peak 1, labda-7,13*E*-dienyl diphosphate; peak 2, *ent*-CPP; and peak 3, GGPP. Bottom panel, compound mass spectrum; middle panel, magnified compound mass spectrum highlighting low-abundance ions.

We tentatively annotated GrTPS4, based on sequence and phylogenetic position, as an *ent*-kaurene synthase class I diTPS (Figure 3). As suitable prenyl diphosphates substrates, which are formed by class II diTPSs, are not commercially available, we used a coupled assay with the ZmAN2 *ent*-CPP synthase to test the function of GrTPS4. The coupled reaction of ZmAN2 and GrTPS4 afforded a single product which was identified as *ent*-kaurene based on its characteristic MS fragmentation pattern of *m/z* 272(51), 257(100), 229(60), 187(22), 147(35) and 109(23) (Figure 5). Additional combinatorial assays of GrTPS2 with GrTPS4 or GrTPS6 did not result in detectable product formation, suggesting that GrTPS2 does not functionally interact with any of the known class I diTPSs in *G. robusta* (Figure 5).

### Transient co-expression of *G. robusta* diTPS in *Nicotiana benthamiana*

To verify the GrTPS2 activity as observed in coupled *in vitro* assays with additional *in vivo* assays, we used *Agrobacterium*-mediated transient (co-)expression in tobacco (*Nicotiana benthamiana*) to investigate combined diTPS activities. For this purpose, FL constructs of GrTPS2 (identified *in vitro* as labda-7,13*E*-dienyl diphosphate synthase) and ZmAN2 (*ent*-CPP synthase) were expressed individually or in combination with the class I diTPSs GrTPS4 (*ent*-kaurene synthase) or GrTPS6 (manoyl oxide synthase). In addition, all combinations were co-expressed with the protein p19 to suppress RNA silencing (Voinnet *et al.*, 2003). The observed *in vivo* products confirmed the *in vitro* enzyme activities (Figure S2). Expression of ZmAN2 and GrTPS4 alone resulted in the formation of *ent*-copalol and labda-7,13*E*-dien-15-ol respectively, indicating the prenyl diphosphate products are metabolized by endogenous phosphatases in *N. benthamiana.* Co-expression of ZmAN2 and GrTPS4 afforded *ent*-kaurene consistent with the results of *in vitro* assays. Conversely, no detectable product formation was observed when expressing GrTPS2 with GrTPS4, supporting a role of GrTPS4 as a product-specific *ent*-kaurene synthase concurrent with known diTPSs involved in GA biosynthesis (Xu *et al.*, 2007; Zhou *et al.*, 2012; Shimane *et al.*, 2014; Zerbe *et al.*, 2014). Co-expression of GrTPS2 with GrTPS6 also yielded no detectable product, whereas an abietadiene-type product was formed by the sequential activity of ZmAN2 and GrTPS6 as previously described (Zerbe *et al.*, 2013).

### Transcript abundance analysis

Transcript levels of diTPSs were measured by quantitative reverse transcription PCR (qRT-PCR) in roots, stems, leaves and whole flowers of *G. robusta* (Figure 6). Transcripts of the *ent*-kaurene synthase *GrTPS4* and the previously characterized manoyl oxide synthase *GrTPS6* were detected across all organs, the latter in agreement with the presence

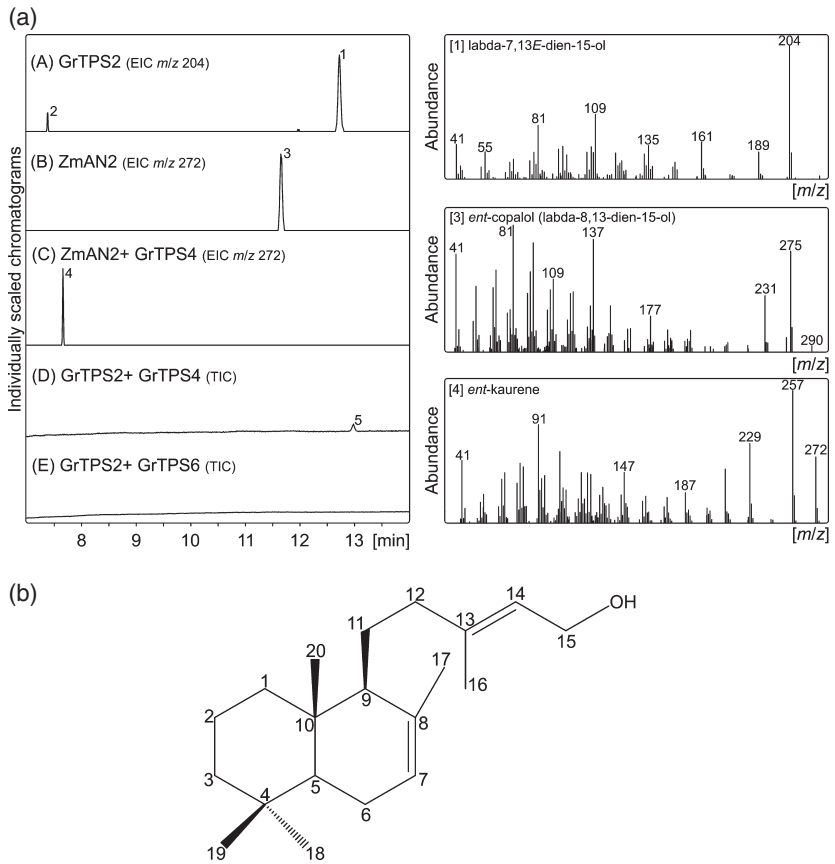


**Figure 5.** GC/MS analysis of GrTPS2 and GrTPS4 reaction products.
(a) GC/MS analysis of reaction products obtained from *in vitro* enzyme assays of recombinant GrTPS2 and GrTPS4 with GGPP as a substrate. Results are illustrated as total (TIC) or extracted (EIC) ion chromatograms (left panels and corresponding mass spectra (right panels).
(aA) Dephosphorylated reaction product of GrTPS2.
(aB) Dephosphorylated *ent*-CPP formed by ZmAN2 (Harris *et al.*, 2005).
(aC) Formation of *ent*-kaurene through the coupled reaction of ZmAN2 and GrTPS4.
(aD, aE) Combined activity of GrTPS2 with GrTPS4 or GrTPS6 (Zerbe *et al.*, 2013), respectively. Peak 1, labda-7,13*E*-dien-15-ol (dephosphorylated labda-7,13*E*-dienyl diphosphate); peak 2, degradation product of labda-7,13*E*-dien-15-ol; peak 3, *ent*-copalol (dephosphorylated *ent*-CPP); and peak 4, *ent*-kaurene; peak 5, plasticizer contamination.
(b) Highlighted is the structure of the dephosphorylated reaction product of GrTPS2 identified as labda-7,13*E*-dien-15-ol (dephosphorylated labda-7,13*E*-dienyl diphosphate) by NMR analysis: $^{1}$H-NMR (600 MHz, MeOD): 5.39 (1H, br s, H-7), 5.36 (1H, t, $J$ = 6.8 Hz, H-14), 4.08 (1H, d, $J$ = 6.8 Hz, H-15), 1.70 (3H, br s, H-17), 1.68 (3H, br s, H-16), 0.90 (3H, s, H-19), 0.87 (3H, s, H-18), 0.79 (3H, s, H-20). $^{13}$C-NMR (MeOD): δ 139.8 (1C, C-13), 136.2 (1C, C-8), 125.0 (1C, C-14), 122.9 (1C, C-7), 59.0 (1C, C-15), 55.5 (1C, C-9), 51.3 (1C, C-5), 43.3 (1C, C-3), 43.2 (1C, C-12), 40.2 (1C, C-1), 37.7 (1C, C-10), 26.3 (1C, C-11), 33.6 (1C, C-4), 33.5 (1C, C-18), 24.7 (1C, C-6), 22.2 (1C, C-17), 22.1 (1C, C-19), 19.5 (1C, C-2), 16.3 (1C, C-16), 13.7 (1C, C-20).

of manoyl oxide in leaves and flowers and to lesser extent also in stem and root tissue. In contrast, transcripts of the LPP synthase *GrTPS1* and the labda-7,13*E*-dienyl diphosphate synthase *GrTPS2* showed organ-specific transcript abundance predominantly in leaves and flowers, while only at trace levels in stems and roots. Furthermore, gene expression levels of *GrTPS2* were six-fold higher in flowers as compared with leaves, in agreement with the higher abundance of grindelic acid in flowers.

## DISCUSSION

Grindelic acid and related labdane diterpenoids, collectively known as grindelanes, are signature metabolites of the genus *Grindelia* that accumulate as a resinous exudate covering the aerial parts of the plant (Bohlmann *et al.*, 1982; Mahmoud *et al.*, 2000) (Figure 1). Although the resinous grindelane secretions may act as a physical and chemical protectant of the inflorescence, such an ecological function has not yet been tested in *Grindelia.* Recent work on *Grindelia* and its diterpenoids, has been motivated by its traditional use as a medicinal plant, and the potential application of grindelane diterpenoids and their synthetic derivatives in cancer therapy and treatment of Alzheimer's disease (Reta *et al.*, 2013; Alza *et al.*, 2014).

### *Grindelia robusta* contains a functionally diverse diTPS family

This study builds on a recently described transcriptome-enabled approach for diterpene pathway discovery in

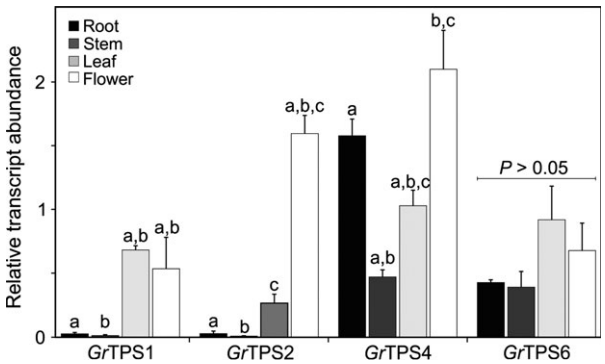


**Figure 6.** Organ-specific transcript abundance of *Grindelia robusta* diterpene synthases.
Transcript abundance was measured by qRT-PCR and normalized to β-tubulin as internal reference. Error bars represent standard errors (SE) based on triplicate measurements of three biological replicates. Statistically significant differences in the organ-specific transcript abundance of individual diTPSs were calculated using a one-way ANOVA test ($P < 0.05$) and are depicted with the letters a, b, and c.

non-model plants, which led to the discovery of six *G. robusta* diTPSs, three of which were characterized as GrTPS1 labda-13-en-8-ol diphosphate synthase, GrTPS5 geranyllinalool synthase, and the multi-functional class I diTPS GrTPS6 (Zerbe *et al.*, 2013). Here, we functionally characterized two additional diTPSs of *G. robusta*, GrTPS4 *ent*-kaurene synthase and GrTPS2 labda-7,13*E*-dienyl diphosphate synthase. With at least six functionally distinct members, the *G. robusta* diTPS family appears to have undergone an extensive evolutionary expansion through gene duplication and neo-functionalization of ancestral diTPSs of general metabolism (Peters, 2010).

*In vitro* and *in vivo* functional characterization paired with phylogenetic analysis (Figure 3) identified GrTPS4 as an *ent*-kaurene synthase (Figures 3, 5 and S2). Transcript patterns (Figure 6) and lack of function of GrTPS4 in coupled assays with the enzymes GrTPS1 and GrTPS2 involved in specialized metabolism (Figure S2) support a role of GrTPS4 in gibberellin biosynthesis. Although GrTPS3 could not be obtained as a FL sequence for functional characterization, BLAST analysis predicted an *ent*-CPP synthase activity, presumably functioning consecutively with GrTPS4 in general metabolism. In contrast, GrTPS2 was characterized as a labda-7,13*E*-dienyl diphosphate synthase of specialized metabolism, consistent with its close phylogenetic relationship with the previously characterized LPP synthase GrTPS1 (Figure 3). Together with the LPP synthase (GrTPS1) and manoyl oxide synthase (GrTPS6) (Zerbe *et al.*, 2013), GrTPS2 and GrTPS4 form the enzymatic foundation for the chemical diversity of labdane diterpenoids in *G. robusta* (Figure 1).

### Labda-7,13*E*-dienyl diphosphate synthase activity evolved independently in distinct species

The catalytic activity of the *Grindelia* labda-7,13*E*-dienyl diphosphate synthase plausibly involves the protonation-initiated bicyclization of GGPP into the intermediate labda-13-en-8-yl$^{+}$ cation, followed by deprotonation of the carbocation at the endocyclic methylene at C-7, as opposed to the more common deprotonation at C-8, to yield CPP (Peters, 2010) (Figure 1). This particular class II reaction has not previously been described for an angiosperm class II diTPS and, to the best of our knowledge, the only other diTPS catalyzing this reaction is the bifunctional class I/II labda-7,13*E*-dien-15-ol synthase SmCPSKSL1 from *S. moellendorffii* (Mafu *et al.*, 2011). However, <50% sequence identity of the SmCPSKSL1 and GrTPS2 class II active sites suggest that biosynthesis of labda-7,13*E*-dienyl diphosphate evolved independently in distant branches of the plant kingdom. This hypothesis is further supported by the occurrence of labdane diterpenoids with a characteristic 7,13 double bond configuration in several taxa, including members of the Verbenaceae, Solanaceae and Zingiberaceae (Reddy *et al.*, 2009; Pérez-Castorena *et al.*, 2010; Hanson, 2011). In species of *Grindelia*, the GrTPS2 function likely evolved early in the speciation given the broad distribution of 7,13-dien diterpenoids across the genus. Indeed, transcriptome analysis of leaf tissue of a related species, *G. integrifolia* (accession no. SRX096932), revealed two GrTPS2 orthologs with protein sequence identity of >99% (Figure S1).

### GrTPS2 functions in grindelic acid biosynthesis

Presence of the 7-8 endocyclic double bond in labda-7,13*E*-dienyl diphosphate suggests that GrTPS2 is a central enzyme in the biosynthesis of grindelic acid and related grindelane diterpenoids (Figure 1). This is further supported by the predominant abundance of *GrTPS2* transcript in leaves and flowers consistent with the high abundance of grindelic acid in these organs (Figures 2 and 6). Despite a 60-fold lower transcript abundance, *GrTPS2* was also expressed in roots accompanied by the presence of trace amounts of grindelic acid, indicating that diterpenoid biosynthesis may also be active in roots of *G. robusta.*

### Grindelic acid biosynthesis may lack a class I diTPS reaction

Despite the previously demonstrated substrate promiscuity of GrTPS6 *in vitro*, no functional interaction with GrTPS2 was observed. *In vitro* and *in vivo* combinatorial assays of GrTPS2 and GrTPS4 also did not result in any detectable product formation (Figures 5 and S2), which raises the question as to which class I diTPS is involved in the conversion of labda-7,13*E*-dienyl diphosphate en route to

grindelic acid. It must be considered that the existing flower-specific transcriptome database did not reveal all *G. robusta* class I diTPSs. This idea is also supported by the fact that the putative *ent*-CPP synthase GrTPS3 was represented by only a short fragment in the transcriptome resource (Figure S1). Alternatively, it can be hypothesized that labda-7,13*E*-dienyl diphosphate is converted by a phosphatase activity to produce labda-7,13*E*-dien-15-ol. Dephosphorylation of the products of ZmAN2, GrTPS1 and GrTPS2 when expressed in *N. benthamiana* illustrate the possibility for such a metabolic fate (Figure S2), and a similar phosphatase-mediated pathway has previously been suggested for diterpenoid formation in *Nicotiana tabacum* (Sallaud *et al.*, 2012). Labda-7,13*E*-dien-15-ol, as potentially produced by sequential activity of GrTPS2 and a phosphatase, could be converted into grindelic acid through P450-catalyzed modifications, including carboxylation at C-15 and formation of the characteristic 9-13 spiroether (Figure 1).

## CONCLUSIONS

In conclusion, the functional characterization of GrTPS2 as a labda-7,13*E*-dienyl diphosphate synthase deepens our knowledge of the lineage-specific evolutionary diversification of diterpenoid metabolism across the plant kingdom. This expanded diTPS functional landscape increases the scope of opportunities for bio-based manufacturing of broader-spectrum diterpenoid bioproducts with potential applications as pharmaceuticals such as grindelic acid and its (semi)-synthetic derivatives.

## EXPERIMENTAL PROCEDURES

### Plant material

Seeds of *G. robusta* were purchased from B&T World Seeds (www.b-and-t-world-seeds.com) and cultivated in a greenhouses under ambient photoperiod with a day temperature of 22°C and a night temperature of 17°C. Seeds of *N. benthamiana* were kindly provided by Dr Katayoon Dehesh (University of California, Davis, USA). Plants were grown in a Conviron PGR15 growth chamber under long-day conditions (16 h light at 80 μmol $m^{-2}$ $sec^{-1}$ irradiance) and a 24°C/17°C day/night temperature.

### Metabolite analysis

Metabolite extracts were prepared from 25–50 mg fresh tissue of flowering plants by pulverization in liquid $N_2$ and subsequent extraction with 1 ml diethyl ether over night at 4°C and under vigorous shaking. Residual water was removed using anhydrous $Na_2SO_4$, followed by filtration through 0.22-μm hydrophilic polypropylene membrane filters (www.pall.com). Due to the high resin acid content of *G. robusta*, samples were further derivatized. Here, a volume of 500 μl of extract was transferred to a fresh vial and incubation at room temperature for 30 min after addition of 100 μl of methanol and 120 μl of trimethylsilyl-diazomethane (2 M in diethyl ether; www.sigma.com). Methylated samples were concentrated under $N_2$ stream and adjusted to 500 μl total volume with diethyl ether prior to GC/MS analysis. Compound identification was performed on an Agilent (www.chem.agilent.com) 6890A GC with a 5975 Inert XL MS Detector at 70 eV and 1.2 ml $min^{-1}$ He flow, using a SGE Solgel-Wax column (30 m, 250 μm i.d., 0.25 μm film; SGE Analytical Science, Austin, TX, USA) and the following GC program: 40°C for 3 min, 8°C $min^{-1}$ to 120°C, 15°C $min^{-1}$ to 250°C, hold 8 min with pulsed splitless injection at 250°C. In addition, head space analysis of volatile terpenoids was performed with 0.5–1 g of whole flowers and leaves. Samples were equilibrated at 85°C for 10 min prior to GC/MS analysis on a 6890A GC with a HP7694 headspace autosampler and a 5975 Inert XL MS Detector using a Agilent DB-Wax column (60 m, 250 μm i.d., 0.25 μm film) and the following conditions: 40°C for 5 min, 5°C $min^{-1}$ to 100°C, 3°C $min^{-1}$ to 200°C, 20°C $min^{-1}$ to 240°C, hold 1 min with a split injector held at 250°C. Metabolite identification is based on significant matches to reference mass spectral databases of the National Institute of Standards and Technology (NIST) MS library searches (Wiley W9N08L). Analyses were carried out in duplicate with three biological replicates and 1-eicosene (Sigma) as an internal standard.

### Isolation and cloning of FL cDNAs

Amplification of cDNAs was done with total RNA from flowers of *G. robusta* using gene-specific oligonucleotides (Table S2). Amplicons were ligated into the pJET vector (www.clontech.com) and verified by sequencing. For expression in *E. coli*, the full-length (FL) cDNA of *GrTPS4* and an N–terminally truncated form of *GrTPS2* (lacking the plastidial signal peptide (Δ47) as predicted based on manual sequence comparison) were subcloned into the expression vector pET28b(+) (www.emdmillipore.ca). Alternatively, for co-expression of diTPSs in *N. benthamiana*, FL cDNAs of *GrTPS4* and *GrTPS2* were amplified and transferred into the pLIFE33 vector (kindly provided by Dr Nour-Eldin, University of Copenhagen, Denmark) by USER cloning.

### Phylogenetic analysis

Protein sequence alignments were generated using the DIALIGN 2.2.1 server (Morgenstern, 2014) and further curated using G blocks (Talavera and Castresana, 2007). Maximum-likelihood phylogenetic analyses were performed using PhyML-aBayes version 3.0.1 beta (Guindon *et al.*, 2010) with four rate substitution categories, LG substitution model, BIONJ starting tree and 1000 bootstrap repetitions.

### Quantitative real-time PCR (qPCR) analysis

Total RNA was prepared as previously described (Kolosova *et al.*, 2014) using approximately 100 mg tissue. RNA integrity and concentration was measured using Bioanalyzer 2100 RNA Nano chip assays (Agilent) according to the supplier's recommendations. Synthesis of cDNAs was performed from equal RNA amounts using Superscript III reverse transcriptase (www.invitrogen.com) and random hexamer oligonucleotides. Quantitative RT-PCR reactions were performed on a Bio-Rad CFX96 Real-time instrument using the SsoFast kit (www.bio-rad.com) and target-specific oligonucleotides (Table S2). Relative transcript abundance was evaluated using efficiency corrected $\Delta C_T$ and $\Delta\Delta C_T$ values based on β–tubulin as reference gene and triplicate measurements with three biological replicates. Significant differences of tissue-specific transcript levels of individual genes were calculated using a one-way analysis of variance (ANOVA) test (*P*-value <0.05) and are depicted as letters a, b, and c. Target specificity was validated by sequence verification of representative amplicons.

 

### *In vitro* enzyme assays

Constructs of GrTPS2 and GrTPS4 in pET28b(+) were transformed into *E. coli* BL21DE3-C41 cells for heterologous expression and $Ni^{2+}$-affinity purification as previously described (Zerbe *et al.*, 2013). Single and coupled diTPS enzyme assays were performed as reported earlier, using 50 μg of recombinant protein and 15 μM of (*E*,*E*,*E*)-GGPP (Sigma) as substrate with gentle shaking for 1 h at 30°C (Zerbe *et al.*, 2013). For LC/MS analysis of the GrTPS2 activity, the reaction product was dephosphorylated by treatment with 10 U of calf intestinal phosphatase (Invitrogen) over night at 37°C prior to metabolite extraction with 500 μl pentane. GC/MS analysis was performed as described above, but with a modified temperature program: 50°C for 1 min, 35°C $min^{-1}$ to 250°C, hold 10 min with pulsed splitless injection at 250°C. LC/MS analysis was conducted on an Agilent 1100 LC/MSD Trap XCT Plus mass spectrometer. Compounds were separated on an Agilent Zorbax SB-C18 column (150 mm × 4.6 mm i.d., 1.8 μm) with isocratic elution at a flow rate of 0.8 ml $min^{-1}$ and 35°C using $NH_4COOCH_3$ as a mobile phase. Mass spectrometric analysis was carried out after electrospray ionization (ESI) in negative mode with a scan range of *m*/*z* 100–600.

### *In vivo* co-expression in *Nicotiana benthamiana*

FL cDNA constructs in the pLIFE33 vector were transformed into *Agrobacterium tumefaciens* strain LBA4404, and cells were grown at 28°C in Luria-Bertani medium supplemented with kanamycin, rifampicin and gentamicin (50 mg $L^{-1}$ each). Cells were then pelleted and resuspended to a final $OD_{600}$ of 0.5 in 10 mM MES buffer with 10 mM $MgCl_2$. Cell suspensions were mixed with one volume of the plant viral protein p19-strain to suppress RNA silencing (Voinnet *et al.*, 2003) for single construct transformations, or using equal volumes for coupled expression with one volume of p19. Following 1 h incubation at 22°C and gentle shaking, the abaxial side of the leaves of 6–week-old *N. benthamiana* plants were infiltrated. Metabolite extraction from transfected plants was performed after 5 days using 1.5 ml hexane from a single transformed leaf and analyzed via GC/MS on an Agilent 7890B GC with a 5977 Extractor XL MS Detector at 70 eV and 1.2 ml $min^{-1}$ He flow, using a HP5-ms column (30 m, 250 μm i.d., 0.25 μm film) and the following GC parameters: 50°C for 1 min, 35°C $min^{-1}$ to 300°C, hold 4 min with pulsed splitless injection at 250°C.

### Nuclear magnetic resonance (NMR) analysis

For NMR analysis, the GrTPS2 product was produced using several *in vitro* assays as described above, with dephosphorylation over night at 37°C. The reaction product was further purified through iterative separation on silica matrix with hexane as mobile phase. NMR analysis was carried out at Sequoia Sciences (www.sequoiasciences.com). Proton, gCOSY, ROESY, gHSQC, and gHMBC NMR spectra were acquired in (deuterated methanol (CD3OD)) at 600 MHz on a Bruker Avance 600 MHz spectrometer equipped with a Bruker BioSpin TCI 1.7 mm MicroCryoProbe. hetereonuclear single quantum coherence and heteronuclear multiple bond correlation spectra were used to obtain $^{13}C$ chemical shifts.

### Accession numbers

Nucleotide sequences described in this study have been deposited to the National Center for Biotechnology Information (NCBI) GenBank™/EBI Data Bank with the following accession numbers: GrTPS2 (KR089902), GrTPS4 (KR089903), GiTPS2A (KR089904) and GiTPS2B (KR089905).

## ACKNOWLEDGEMENTS

We thank Ms Karen Reid (University of British Columbia) for excellent laboratory and project management support, and Ms Lina Madilao (University of British Columbia) for support with metabolite analysis. We gratefully acknowledge Dr Johan Memelink (Leiden University, The Netherlands) for providing the *A. tumefaciens* strain LBA4404. We further thank Dr Björn Hamberger (University of Copenhagen, Denmark) for providing the pLIFE33 and pLIFE33-ZmAN2 plasmids, and Dr David Baulcombe (University of Cambridge, UK) for sharing the p19 plasmid. Financial support was provided by the Natural Sciences and Engineering Research Council of Canada (NSERC; to JB) and funds in support of the PhytoMetaSyn Project (to JB) from Genome Canada, Genome Alberta, Government of Alberta, Genome British Columbia, Genome Prairie, Genome Quebec, National Research Council of Canada, Canada Foundation for Innovation, Ontario Ministry of Research and Innovation, McGill Innovation Centre, MDEIE (Ministere du Developement Economique, Innovation et Exportation) and other government and private sector partners. JB is a University of British Columbia Distinguished University Scholar. PZ acknowledges financial support by the College of Biological Sciences at the University of California at Davis, USA.

## CONFLICT OF INTEREST STATEMENT

The authors declare that they have no conflict of interest in accordance with the journal policy.

## SUPPORTING INFORMATION

Additional Supporting Information may be found in the online version of this article.

**Figure S1.** Protein sequence alignment of class II diTPS from *Grindelia robusta* and the leaf.

**Figure S2.** Diterpene synthase co-expression in *Nicotiana benthamiana.*

**Table S1.** Tissue-specific metabolite profile of *Grindelia robusta.*

**Table S2.** Oligonucleotides used in this study.

## REFERENCES

**Ahmed, A.A., Mahmoud, A.A., Ahmed, U.M., El-Bassuony, A.A., Abd El-Razk, M.H., Pare, P.W. and Karchesy, J.** (2001) Manoyl oxide alpha-arabinopyranoside and grindelic acid diterpenoids from *Grindelia integrifolia*. *J. Nat. Prod.* **64**, 1365–1367.

**Alza, N.P., Richmond, V., Baier, C.J., Freire, E., Baggio, R. and Murray, A.P.** (2014) Synthesis and cholinesterase inhibition of cativic acid derivatives. *Bioorg. Med. Chem.* **22**, 3838–3849.

**Bartoli, A., Galati, B.G. and Tortosa, R.D.** (2011) Anatomical studies of the secretory structures: Glandular trichomes and ducts, in *Grindelia pulchella* Dunal (Astereae, Asteraceae). *Flora*, **206**, 1063–1068.

**Bohlmann, J. and Keeling, C.I.** (2008) Terpenoid biomaterials. *Plant J.* **54**, 656–669.

**Bohlmann, F., Ahmed, M., Borthakur, N., Wallmeyer, M., Jakupovic, J., Kinga, R.M. and Robinson, H.** (1982) Diterpenes related to grindelic acid and further constituents from *Grindelia* species. *Phytochemistry*, **21**, 167–172.

**Brückner, K., Božić, D., Manzano, D., Papaefthimiou, D., Pateraki, I., Scheler, U., Ferrer, A., de Vos, R.C., Kanellis, A.K. and Tissier, A.** (2014) Characterization of two genes for the biosynthesis of abietane-type diterpenes in rosemary (*Rosmarinus officinalis*) glandular trichomes. *Phytochemistry*, **101**, 52–64.

**Chen, F., Tholl, D., Bohlmann, J. and Pichersky, E.** (2011) The family of terpene synthases in plants: a mid-size family of genes for specialized metabolism that is highly diversified throughout the kingdom. *Plant J.* **66**, 212–229.

**Davis, E.M. and Croteau, R.** (2000) Cyclization enzymes in the biosynthesis of monoterpenes, sesquiterpenes, and diterpenes. In *Topics in Current Chemistry: Biosynthesis: Aromatic Polyketides, Isoprenoids, Alkaloids* (Leeper, F.J. and Vederas, J.C. eds). Berlin, Springer, pp. 53–95.

**Facchini, P.J., Bohlmann, J., Covello, P.S., De Luca, V., Mahadevan, R., Page, J.E., Ro, D.-K., Sensen, C.W., Storms, R. and Martin, V.J.J.** (2012) Synthetic biosystems for the production of high-value plant metabolites. *Trends Biotechnol.* **30**, 127–131.

**Falara, V., Pichersky, E. and Kanellis, A.K.** (2010) A copal-8-ol diphosphate synthase from the angiosperm *Cistus creticus* subsp. creticus is a putative key enzyme for the formation of pharmacologically active, oxygen-containing labdane-type diterpenes. *Plant Physiol.* **154**, 301–310.

**Fraternale, D., Giamperi, L., Bucchini, A. and Ricci, D.** (2007) Essential oil composition and antioxidant activity of aerial parts of *Grindelia robusta* from Central Italy. *Fitoterapia*, **78**, 443–445.

**Gershenzon, J. and Dudareva, N.** (2007) The function of terpene natural products in the natural world. *Nat. Chem. Biol.* **3**, 408–414.

**Guindon, S., Dufayard, J.F., Lefort, V., Anisimova, M., Hordijk, W. and Gascuel, O.** (2010) New algorithms and methods to estimate maximum-likelihood phylogenies: assessing the performance of PhyML 3.0. *Syst. Biol.* **59**, 307–321.

**Hanson, J.R.** (2011) Diterpenoids of terrestrial origin. *Nat. Prod. Rep.* **28**, 1755–1772.

**Harris, L.J., Saparno, A., Johnston, A., Prisic, S., Xu, M., Allard, S., Kathiresan, A., Ouellet, T. and Peters, R.J.** (2005) The maize An2 gene is induced by *Fusarium* attack and encodes an *ent*-copalyl diphosphate synthase. *Plant Mol. Biol.* **59**, 881–894.

**Harvey, A.L., Edrada-Ebel, R. and Quinn, R.J.** (2015) The re-emergence of natural products for drug discovery in the genomics era. *Nat. Rev. Drug Discov.* **14**, 111–129.

**Higashi, Y. and Saito, K.** (2013) Network analysis for gene discovery in plant-specialized metabolism. *Plant Cell Environ.* **36**, 1597–1606.

**Keeling, C.I. and Bohlmann, J.** (2006a) Diterpene resin acids in conifers. *Phytochemistry*, **67**, 2415–2423.

**Keeling, C.I. and Bohlmann, J.** (2006b) Genes, enzymes and chemicals of terpenoid diversity in the constitutive and induced defence of conifers against insects and pathogens. *New Phytol.* **170**, 657–675.

**Keeling, C.I., Dullat, H.K., Yuen, M., Ralph, S.G., Jancsik, S. and Bohlmann, J.** (2010) Identification and functional characterization of monofunctional *ent*-copalyl diphosphate and *ent*-kaurene synthases in white spruce reveal different patterns for diterpene synthase evolution for primary and secondary metabolism in gymnosperms. *Plant Physiol.* **152**, 1197–1208.

**Kolosova, N., Breuil, C. and Bohlmann, J.** (2014) Cloning and characterization of chitinases from interior spruce and lodgepole pine. *Phytochemistry*, **101**, 32–39.

**Mafu, S., Hillwig, M.L. and Peters, R.J.** (2011) A novel labda-7,13*E*-dien-15-ol-producing bifunctional diterpene synthase from *Selaginella moellendorffii*. *Chembiochem*, **12**, 1984–1987.

**Mahmoud, A.A., Ahmed, A.A., Tanaka, T. and Iinuma, M.** (2000) Diterpenoid acids from *Grindelia nana*. *J. Nat. Prod.* **63**, 378–380.

**Morgenstern, B.** (2014) Multiple sequence alignment with DIALIGN. *Methods Mol. Biol.* **1079**, 191–202.

**Nelson, D. and Werck-Reichhart, D.** (2011) A P450-centric view of plant evolution. *Plant J.* **66**, 194–211.

**Pateraki, I., Andersen-Ranberg, J., Hamberger, B., Heskes, A.M., Martens, H.J., Zerbe, P., Bach, S.S., Møller, B.L., Bohlmann, J. and Hamberger, B.** (2014) Manoyl oxide (13*R*), the biosynthetic precursor of forskolin, is synthesized in specialized root cork cells in *Coleus forskohlii*. *Plant Physiol.* **164**, 1222–1236.

**Pérez-Castorena, A.-L., Martínez, M. and Maldonado, E.** (2010) Labdanes and sucrose esters from *Physalis sordida*. *J. Nat. Prod.* **73**, 1271–1276.

**Peters, R.J.** (2010) Two rings in them all: the labdane-related diterpenoids. *Nat. Prod. Rep.* **27**, 1521–1530.

**Pugliesi, C., Fambrini, M. and Salvini, M.** (2011) Molecular cloning and expression profile analysis of three sunflower (*Helianthus annuus*) diterpene synthase genes. *Biochem. Genet.* **49**, 46–62.

**Reddy, P.P., Rao, R.R., Shashidhar, J., Sastry, B.S., Rao, J.M. and Babu, K.S.** (2009) Phytochemical investigation of labdane diterpenes from the rhizomes of *Hedychium spicatum* and their cytotoxic activity. *Bioorg. Med. Chem. Lett.* **19**, 6078–6081.

**Reta, G.F., Chiaramello, A.I., García, C., León, L.G., Martín, V.S., Padrón, J.M., Tonn, C.E. and Donadel, O.J.** (2013) Derivatives of grindelic acid: from a non-active natural diterpene to synthetic antitumor derivatives. *Eur. J. Med. Chem.* **67**, 28–38.

**Richman, A.S., Gijzen, M., Starratt, A.N., Yang, Z. and Brandle, J.E.** (1999) Diterpene synthesis in *Stevia rebaudiana:* recruitment and up-regulation of key enzymes from the gibberellin biosynthetic pathway. *Plant J.* **19**, 411–421.

**Sallaud, C., Giacalone, C., Töpfer, R., Goepfert, S., Bakaher, N., Rösti, S. and Tissier, A.** (2012) Characterization of two genes for the biosynthesis of the labdane diterpene *Z*-abienol in tobacco (*Nicotiana tabacum*) glandular trichomes. *Plant J.* **72**, 1–17.

**Sawada, Y., Katsumata, T., Kitamura, J. *et al.*** (2008) Germination of photoblastic lettuce seeds is regulated via the control of endogenous physiologically active gibberellin content, rather than of gibberellin responsiveness. *J. Exp. Bot.* **59**, 3383–3393.

**Shimane, M., Ueno, Y., Morisaki, K., Oogami, S., Natsume, M., Hayashi, K., Nozaki, H. and Kawaide, H.** (2014) Molecular evolution of the substrate specificity of *ent*-kaurene synthases to adapt to gibberellin biosynthesis in land plants. *Biochem. J.* **462**, 539–546.

**Talavera, G. and Castresana, J.** (2007) Improvement of phylogenies after removing divergent and ambiguously aligned blocks from protein sequence alignments. *Syst. Biol.* **56**, 564–577.

**Veres, K., Roza, O., Laczkó-Zöld, E. and Hohmann, J.** (2014) Chemical composition of essential oils of *Grindelia squarrosa* and *G. hirsutula*. *Nat. Prod. Commun.* **9**, 573–574.

**Voinnet, O., Rivas, S., Mestre, P. and Baulcombe, D.** (2003) An enhanced transient expression system in plants based on suppression of gene silencing by the p19 protein of tomato bushy stunt virus. *Plant J.* **33**, 949–956.

**Xu, M., Wilderman, P.R., Morrone, D., Xu, J., Roy, A., Margis-Pinheiro, M., Upadhyaya, N.M., Coates, R.M. and Peters, R.J.** (2007) Functional characterization of the rice kaurene synthase-like gene family. *Phytochemistry*, **68**, 312–326.

**Ybarra, M.I., Popich, S., Borkosky, S.A., Asakawa, Y. and Bardón, A.** (2005) Manoyl oxide diterpenoids from *Grindelia scorzonerifolia*. *J. Nat. Prod.* **68**, 554–558.

**Zerbe, P. and Bohlmann, J.** (2015a) Plant diterpene synthases: exploring modularity and metabolic diversity for bioengineering. *Trends Biotechnol.* **33**, 419–428.

**Zerbe, P. and Bohlmann, J.** (2015b) Enzymes for synthetic biology of ambroxide-related diterpenoid fragrance compounds. *Adv. Biochem. Eng. Biotechnol.* **48**, 427–447.

**Zerbe, P., Chiang, A., Yuen, M., Hamberger, B., Hamberger, B., Draper, J.A., Britton, R. and Bohlmann, J.** (2012) Bifunctional *cis*-abienol synthase from *Abies balsamea* discovered by transcriptome sequencing and its implications for diterpenoid fragrance production. *J. Biol. Chem.* **287**, 12121–12131.

**Zerbe, P., Hamberger, B., Yuen, M.M., Chiang, A., Sandhu, H.K., Madilao, L.L., Nguyen, A., Hamberger, B., Bach, S.S. and Bohlmann, J.** (2013) Gene discovery of modular diterpene metabolism in nonmodel systems. *Plant Physiol.* **162**, 1073–1091.

**Zerbe, P., Chiang, A., Dullat, H., O'Neil-Johnson, M., Starks, C., Hamberger, B. and Bohlmann, J.** (2014) Diterpene synthases of the biosynthetic system of medicinally active diterpenoids in *Marrubium vulgare*. *Plant J.* **79**, 914–927.

**Zhou, K., Xu, M., Tiernan, M. *et al.*** (2012) Functional characterization of wheat *ent*-kaurene(-like) synthases indicates continuing evolution of labdane-related diterpenoid metabolism in the cereals. *Phytochemistry*, **84**, 47–55.

 